

QUANTITATIVE FRACTOGRAPHY BY MEANS OF A NEW DIGITAL IMAGE ANALYSIS SYSTEM

O. Kolednik¹, S. Scherer², P. Schwarzböck¹ and P. Werth¹

¹ Erich Schmid Institute of Materials Science, Austrian Academy of Sciences,
A - 8700 Leoben, Austria

² Institute of Computer Graphics and Vision, Technical University Graz,
A - 8010 Graz, Austria

ABSTRACT

A digital image analysis system has been developed that is capable of analyzing automatically stereo image pairs taken in the scanning electron microscope. The key part of the system is a matching algorithm which is able to find homologue points in the two images. The system generates a digital elevation model (DEM) of the depicted region consisting of about 15.000 to 20.000 points. An additional "Roughness Package" allows the direct evaluation of profile and surface roughness parameters. By a variation of the number of points in the DEM, the fractal dimensions can be computed. It is studied how the roughness parameters and the fractal dimensions vary depending on the number of points in the DEM and the magnification of the micrographs. The material is a 6061 aluminum alloy. Important additional capabilities of the automatic fracture surface analysis system are discussed, for instance the determination of local fracture toughness parameters, such as the critical crack tip opening displacement, COD_i , or the crack tip opening angle, COA . By this way, the fracture toughness parameters can be determined locally which is essential for studying the fracture properties of inhomogeneous materials, or for analyzing the constraint effects in homogeneous materials.

INTRODUCTION

For quantitative analyses of fracture surfaces, SEM-stereophotogrammetry is very suitable [1, 2]. The main advantages compared to other possible methods are the high accuracy at arbitrary magnifications, the high depth of focus of the scanning electron microscope (SEM), and the possibility to find corresponding regions on both fracture surfaces which is important for many applications, e.g., for determining the critical crack tip opening displacement (COD_i) [3]. In the past, the main disadvantage of stereophotogrammetry was the long time needed for the analysis made on a stereo comparator [3, 4] or an analytical stereo plotter [5]. The first semi-automatic analyses were reported in [6, 7]. Recently, a new image processing system was developed that permits the fully automatic analysis of stereophotograms [8, 9]. The system yields a so-called "digital elevation model" (DEM) of the depicted fracture surface region consisting of about 15.000 to 20.000 points. It will be demonstrated in this paper that the DEM can be processed to perform a quantitative analysis of the fracture surface: Profile roughness and surface roughness parameters can be extracted, fractal dimensions can be determined and fracture toughness parameters, such as COD_i or the crack tip opening angle (COA), can be measured.

In next section, the system for automatic fracture surface reconstruction is briefly described, followed by a section about the determination of roughness parameters.

THE SYSTEM FOR AUTOMATIC FRACTURE SURFACE RECONSTRUCTION

Stereo image pairs (stereophotograms) are taken in a LEO S440 scanning electron microscope by tilting the specimen by an angle of 10 degrees. The specimen is mounted on a eucentric sample holder so that the tilt axis lies on the specimen surface; consequently, the image does not move during the tilt and the working distance remains constant. To determine the exact magnification, a scale should be photographed at the same working distance. In [4] a procedure is listed how stereophotograms should be taken, also in case that no eucentric sample holder is available. The SEM images have a resolution of 1024x768 points and 256 gray levels.

Our system for automatic fracture surface reconstruction is similar to those used for the analysis of aerial and satellite photographs [10]. The essential part of the system is a matching algorithm which identifies homologue, i.e., corresponding, points on the two stereophotograms. First, we used a hierarchical area based algorithm developed by [11], see [8, 9]. Hereby, the first image is split into many small sub-areas (“windows”), and the matching algorithm tries to find the best position of each window on the second image by comparing the matrices of the gray levels. The center points of the windows in the two images are taken as homologue points. In the meantime, the matching algorithm has been completely reconstructed and greatly improved. The most important improvements are the introduction of an adaptive window size [12], the application of rank based correlation methods (not the absolute size of the gray levels is considered but their relative order) [13], and subpixel strategies [14]. The result is a DEM of the fracture surface region consisting of about 15.000 to 20.000 points with known (x, y, z) co-ordinates. The computation time is about 15 minutes on a fast PC.

The system has a very convenient operating surface where the surfaces can be viewed monoscopically or, with the help of stereo glasses, stereoscopically. This allows the user to check the quality of the matching process, to correct outsiders, to insert additional homologue points, etc.

THE AUTOMATIC DETERMINATION OF ROUGHNESS PARAMETERS

A review of the application of stereophotogrammetry in quantitative fractography is given in [1, 2]; because of the time consuming analysis, the direct determination of the surface roughness is sparse, e.g. [1]. Much more often, the profile roughness has been determined either by stereophotogrammetry or by the analysis of metallographic sections. Therefore, much effort has been made to estimate the surface roughness from the R_L values [1, 2, 15, 16].

An additional program package, “Roughness Package”, has been written to extract roughness parameters from the DEM. A triangulation of all points of the DEM leads to a network of triangles that can be sectioned arbitrarily to draw profiles. The profile roughness is determined as the fraction of the true profile length over the projected profile length in the crack plane [2, 15],

$$R_L = \frac{L}{L'} . \quad (1)$$

Similarly, the surface roughness is determined directly as the true surface area divided by its projected area [2],

$$R_S = \frac{S}{S'} . \quad (2)$$

It should be noted that for randomly oriented segments $R_L = \pi/2 \cong 1.57$, and for randomly oriented surface elements $R_S = 2$, [15]. The Roughness Package allows the operator analyze automatically a certain number of horizontal or vertical profiles, or to mark arbitrary paths or areas where the roughness parameters should be computed.

The apparent length $L(\eta)$ of an irregular profile depends on the size of the measuring unit η [18],

$$L(\eta) = L_0 \eta^{-(D_L-1)} . \quad (3)$$

L_0 is a constant with the dimension of a length, and D_L the fractal dimension of the profile. Similarly, the area of an irregular surface $S(\eta^2)$ is given by

$$S(\eta^2) = S_0 (\eta^2)^{-(D_S-2)/2}, \quad (4)$$

where η^2 is the area measuring unit, S_0 a constant, and D_S the fractal dimension of the surfaces. Equations 3 and 4 can be easily modified to get useful relations to the roughness parameters [19],

$$R_L(\eta) = C_1 \eta^{-(D_L-1)}, \quad (5)$$

and

$$R_S(\eta^2) = C_2 (\eta^2)^{-(D_S-2)/2} = C_2 (\eta)^{-(D_S-2)}. \quad (6)$$

C_1 and C_2 are dimensionless constants. The fractal dimensions can now be computed by determining the roughness parameters on DEMs which have various numbers of points.

In the following section, the power of the new digital image system for quantitative fractography purposes shall be demonstrated.

THE ROUGHNESS PARAMETERS OF A MICRO-DUCTILE FRACTURE SURFACE

Figure 1 shows the fracture surface of a wrought 6061 aluminum alloy that was aged at room temperature. The composition of the material is given in Table 1. The SEM stereophotograms were taken at a low magnification, $M = 29$. DEMs were analyzed with different numbers of points, and for each DEM the roughness parameters were evaluated within the marked area.

TABLE 1
Chemical composition of the Al 6061 alloy

Si	Fe	Cu	Mn	Mg	Zn	Cr	Ti
0.4 – 0.8	0.7	0.15 – 0.4	0.15	0.8 – 1.2	0.25	0.04 – 0.35	0.15

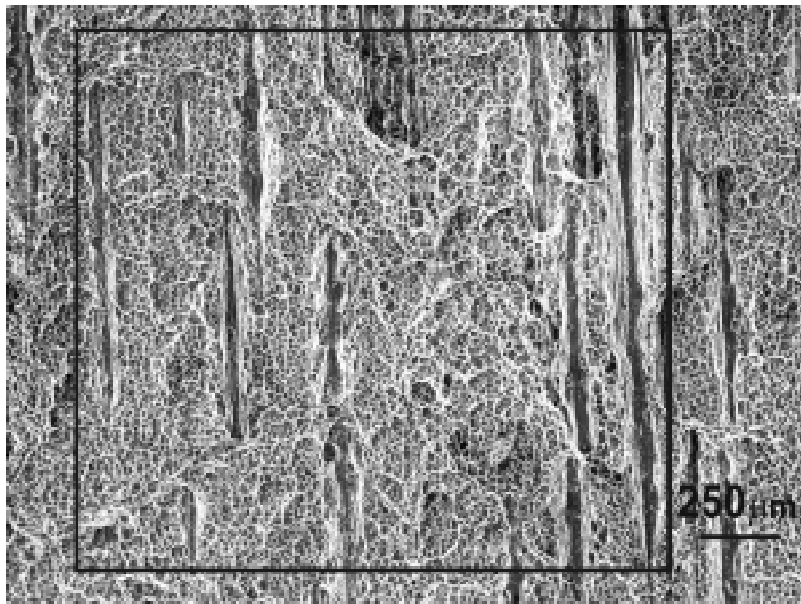


Figure 1: Fracture surface of a wrought Al 6061 taken at a low magnification, $M = 29$.

50 equidistant horizontal and vertical profiles were automatically analyzed to determine the profile roughness in horizontal and vertical direction, $R_{L,hor}$ and $R_{L,verb}$. The results, including the values of the area

roughness, R_s , and the fractal dimensions of the profiles, $D_{L,hor}$ and $D_{L,vert}$, and the area, D_s , are collected in Table 2. The first column lists the number of points of the DEM within the analyzed area.

TABLE 2

Roughness data for different point densities of the DEM and fractal dimensions; low magnification $M = 29$

Points	$R_{L,hor}$	$R_{L,vert}$	R_s	$D_{L,hor}$	$D_{L,vert}$	D_s
2780	1.23	1.14	1.33	1.11	1.08	2.15
5921	1.28	1.17	1.41			
9627	1.31	1.19	1.47			
12534	1.34	1.20	1.49			
17098	1.36	1.22	1.53			

As has been expected, there is no absolute measure of the roughness: the data increase with the number of points in the DEM. Due to the orientation of the material which is clearly visible, the profile roughness and the fractal dimension in the horizontal direction are larger than in the vertical direction.

From the center region of Figure 1, other stereophotograms were taken at higher magnifications $M = 141$. From the marked area of Figure 2, the roughness parameters were evaluated, see Table 3. The values are larger than for $M = 29$. Again, the values increase with the number of points in the DEM, and an orientation dependency is observed although this cannot be seen by the naked eye. The numbers of the fractal dimension come close to those measured for the lower magnification.

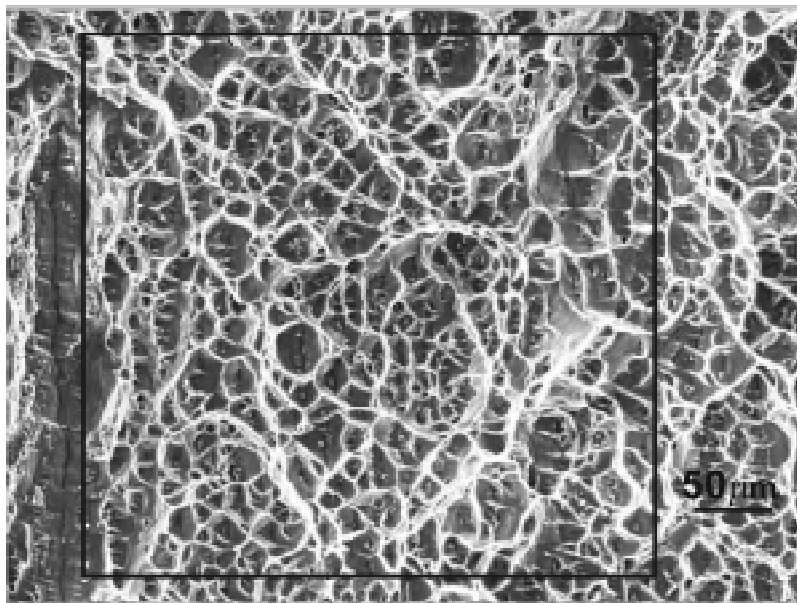


Figure 2: Center region of Figure 1 taken at a higher magnification, $M = 141$.

TABLE 3

Roughness data for different point densities of the DEM and fractal dimensions; high magnification $M = 141$

Points	$R_{L,hor}$	$R_{L,ver}$	R_s	$D_{L,hor}$	$D_{L,vert}$	D_s
2623	1.43	1.38	1.69	1.11	1.09	2.16
5704	1.50	1.42	1.81			
9496	1.53	1.45	1.87			
12507	1.56	1.47	1.93			
17227	1.59	1.50	1.97			

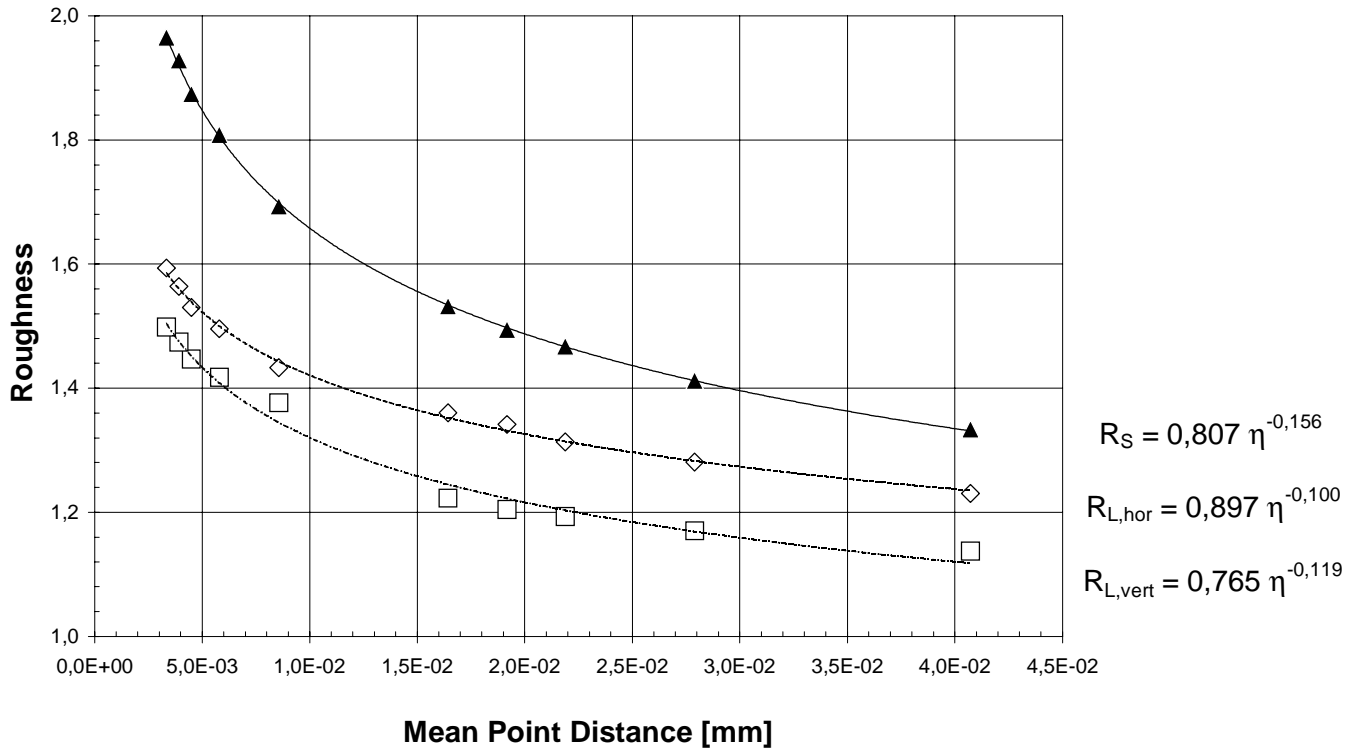


Figure 3: Roughness data of Table 2 and 3 plotted together against the mean point distance η

Both the number of points in the DEM and the magnification determine the size of the measuring unit η for the roughness determination; η can be considered as the mean point distance in the DEM. The points in the DEM are distributed homogeneously, therefore η is calculated as

$$\eta = \sqrt{\frac{S'}{N_S}}, \quad (7)$$

where N_S is the number of points of the DEM within the analyzed area. In Figure 3, the roughness data of Table 2 and 3 together are plotted against the mean point distance η . The R_S data for the five different N_S values and the two different magnifications fall nicely onto a single curve; the fit is not so good for the profile roughness, especially for the vertical profiles. The equations of the best-fit potential curves are also stated in the figure. With Equations 5 and 6, the exponents can be easily transformed into the fractal dimensions that are valid for the whole regime: $D_{L,vert} = 1.12$, $D_{L,hor} = 1.10$ and $D_S = 2.16$. For the horizontal profiles and the surface, almost no difference is seen between the fractal dimensions of the whole η -regime and the partial regions at the two different magnifications. On the contrary, $D_{L,vert}$ of the whole η -regime is notably higher than the values listed in Tables 2 and 3 for the partial regions. The reason is that the orientation effect becomes weaker for higher magnifications and should finally disappear, i.e., the R_L curves for the vertical and the horizontal directions should merge for small η values. (It should be noted that the $D_{L,vert}$ values for the partial regions are nearly equal but the pre-factors in Equation 5 are different.)

In [20], the investigation has been extended to seven different magnifications between $M = 29$ and 760 which corresponds to mean point distances between $\eta = 0.04$ and 0.0007 mm.

ADDITIONAL APPLICATIONS OF A QUANTITATIVE FRACTURE SURFACE INSPECTION

Our system for automatic fracture surface reconstruction is not only useful for measuring roughness parameters, it can be also applied for fracture toughness determination. Stereophotograms are taken from corresponding regions on both halves of a broken specimen and analyzed. From the two DEMs, corresponding profiles perpendicular to the crack front are extracted to measure directly the critical crack tip opening displacement, COD_i , or the critical crack tip opening angle, COA . The procedures are described in [3, 9] for the determination of COD_i , in [21] for the determination of COA .

COD_i is a measure of the fracture initiation toughness, and it can be related to the stress intensity, K_i , or the J-integral, J_i , at fracture initiation. COA is a measure of the crack growth toughness; it is related to the slope of the $J-\Delta a$ curve, or to the crack growth resistance, R , (which is often denoted as energy dissipation rate, D). These relations have been practically applied in [22] where characteristic crack growth resistance terms for flat fracture and shear lip fracture have been evaluated. The advantage of stereophotogrammetry is that the fracture toughness parameters can be determined locally which is essential for analyzing the constraint effects in homogeneous materials, or for studying the fracture properties of inhomogeneous materials.

In the case of an ideally brittle fracture, the DEMs of the corresponding regions would match perfectly like the pieces of a broken vase. If plasticity is involved in the fracture process, a misfit appears between the corresponding DEMs. By arranging properly the corresponding DEMs, a “void map” can be generated which can be used subsequently to estimate the specific fracture surface energy, i.e., the energy to form the dimple structure of a fracture surface [23].

Especially for the analysis of cleavage fracture surfaces, we have developed recently a technique termed the crystallographic fractometry [24]: Stereophotogrammetry is used to measure the orientation of a cleavage plane in space; electron backscatter diffraction (EBSD) yields the crystallographic orientation of the considered crystal. The combination of the two results allows us to determine the crystallographic indices of the cleavage plane and the crystallographic indices of certain direction on the plane. For example, in [25] the method was applied to explore the crystallographic nature of different cleavage planes in a fully lamellar TiAl alloy.

SUMMARY

A digital image analysis system has been developed that is capable of analyzing automatically stereo image pairs taken in the scanning electron microscope. The system generates a digital elevation model (DEM) of the depicted region consisting of about 15.000 to 20.000 points. An additional “Roughness Package” allows the direct evaluation of profile and surface roughness parameters. It was studied how the roughness parameters and the fractal dimensions vary depending on the number of points in the DEM and the magnification of the micrographs. Important additional capabilities of the automatic fracture surface analysis system were discussed, for instance the determination of local fracture toughness parameters such as the critical crack tip opening displacement, COD_i , or the crack tip opening angle, COA . So far, our system has been applied to reconstruct ductile, cleavage, and fatigue fracture surfaces of different sorts of materials such as metals, metal matrix composites, metallic glasses, metallic foams, and intermetallic alloys; it is also possible to analyze the surfaces of biological materials or micro chips.

ACKNOWLEDGEMENTS

The authors acknowledge gratefully the financial support of this work by the Austrian Fonds zur Förderung der wissenschaftlichen Forschung and by the Österreichische Nationalbankfonds under the project number P12278-MAT / FWF 482.

REFERENCES

1. Exner H.E. and M. Fripan (1985) *Journal of Microscopy* **138**, 161.
2. Underwood, E.E. and K. Banerjee, K. (1987). In: *Metals Handbook, Ninth Edition, Volume 12*. ASM International, Metals Park, Ohio, USA, pp.193-210.
3. Kolednik, O. and Stüwe, H.P. (1985) *Engineering Fracture Mechanics* **21**, 145.
4. Kolednik O. (1981) *Practical Metallography* **18**, 562.
5. Bauer B. and A. Haller (1981) *Practical Metallography* **18**, 327.
6. Bryant D. (1986) *Micron Microscopy Acta* **17**, 237.
7. Kobayashi T. and D. A. Shockey (1987) *Metallurgical Transactions* **18A**, 1941.
8. Stampfl, J., Scherer, S., Gruber, M. and Kolednik, O. (1996) *Applied Physics* **A63**, 341.

9. Stampfl, J., Scherer, S., Berchthaler, M., Gruber, M. and Kolednik, O. (1996) *International Journal of Fracture* **78**, 35.
10. Konecny, G. and Lehmann, G. (1984) *Photogrammetry*. Walter de Gruyter, Berlin.
11. Frankot, R.T., Hensley, S. and Shaffer, S. (1994). In: *Proceedings of the International Geoscience and Remote Sensing Symposium*, Caltech Pasadena, CA, pp. 1151-1153.
12. Scherer, S., Andexer, W. and Pinz, A. (1998). In: *Proceedings of the 14th International Conference on Pattern Recognition*, A.K. Jain, S. Venkatesh, B.C. Lowell, Eds., IEEE Computer Society, Los Alamitos, CA, pp. 777-779.
13. Scherer, S., Werth, P. and Pinz, A. (1999). In: *1999 IEEE Computer Society Conference on Computer Vision and Pattern Recognition*, IEEE Computer Society, Los Alamitos, CA, Volume 1, pp. 225-234.
14. Werth, P., Scherer, S. and Pinz, A. (1999). In: *Computer Analysis of Images and Patterns, Proc. of CAIP'99*, F. Solina, A. Leonardis, Eds., Springer Verlag, Berlin, pp. 641-648.
15. Underwood, E.E. (1970) *Quantitative Stereology*. Addison-Wesley, Reading, MA, USA.
16. Wright, K. and Karlsson, B. (1983) *Journal of Microscopy* **130**, 37.
17. Pickens, J.R. and Gurland, J. (1976). In: *Proceedings of the Fourth International Conference of Stereology*, E.E. Underwood, R. de Wit, G.A. Moore, Eds., NBS 431, National Bureau of Standards, pp. 269-272.
18. Mandelbrot, B.B. (1977) *Fractals: Form, Change and Dimension*. Freeman, San Francisco.
19. Underwood, E.E. and K. Banerjee, K. (1987). In: *Metals Handbook, Ninth Edition, Volume 12*. ASM International, Metals Park, Ohio, USA, pp.211-215.
20. Kolednik, O. and Schwarzböck, P., to be published.
21. Shan, G.X., Kolednik, O., Fischer, F.D. and Stüwe, H.P. (1993) *Engineering Fracture Mechanics* **45**, 99.
22. Stampfl, J. and Kolednik, O. (2000) *International Journal of Fracture*, in press.
23. Stampfl J., Scherer, S., Stüwe, H.P. and Kolednik, O. (1996). In: *Mechanisms and Mechanics of Damage and Failure, Proc. Of ECF 11*, J. Petit, Ed., EMAS, UK, Vol.3, pp.1271-1276.
24. Semprinoschnig, C.O.A., Stampfl, J., Pippan, R. and Kolednik, O. (1997) *Fatigue and Fracture of Engineering Materials and Structures* **20**, 1541.
25. Hebesberger, T., Semprinoschnig, C.O.A., Pippan, R., Kolednik, O. and Clemens, H. (1999). In: *Gamma Titanium Aluminides 1999*, Y.-W. Kim, D.M. Dimiduk, M.H. Loretto, Eds., TMS, pp. 573-578.